Regular Article

PHYSICAL CHEMISTRY RESEARCH
Published by the
Iranian Chemical Society
www.physchemres.org
info@physchemres.org

Phys. Chem. Res., Vol. 12, No. 4, 901-918, December 2024
DOI: 10.22036/pcr.2024.444731.2482

Molecular Design and Optoelectronic Investigations of Phenothiazine D-A-π-A Dye-Sensitizers Using DFT/TD-DFT Method for Potential Solar Cell Application

William Ojoniko Anthony[a], K.G. Obiyenwa[a], M.K. Abubakar[c], O.W. Salawu[a,*] and B. Semire[a,b,*]

[a]*Department of Chemistry, Federal University, Lokoja, Kogi State, Nigeria*

[b]*Computational Chemistry Laboratory, Department of Pure and Applied Chemistry, Ladoke Akintola University of Technology, Ogbomoso, Nigeria*

[c]*Department of Science Laboratory Technology, Kogi State Polytechnic, Lokoja, Kogi State, Nigeria*

(Received 19 February 2024, Accepted 1 June 2024)

Renewable energy, like solar energy, has become a viable solution to the scarcity, environmental degradation, and greenhouse effects of fossil fuels. Many technology companies are developing reliable and affordable sustainable energy technology to convert sunlight into electricity and reduce greenhouse gas emissions and nuclear by-products. In this research, eight metal-free organic phenothiazine and phenoxazine-based dyes of the D-A-π-A architecture were studied theoretically using DFT and TD-DFT techniques for use as dye-sensitized solar cells (DSSCs). The effects of π-spacers on the structural, electrical, photovoltaic, and optical characteristics of the designed dyes were examined. The results showed that 2-[3-(10*H*-phenoxazin-3-yl)furan-2-yl]-10*H*-phenoxazine (PO) dyes have lower band gaps (ΔEg) than 2-[3-(10*H*-phenothiazin-3-yl)furan-2-yl]-10*H*-phenothiazine (PZ) dyes, which means 2-[3-(10*H*-phenoxazin-3-yl)furan-2-yl]-10*H*-phenoxazine pushed electrons towards the acceptor unit readily than 2-[3-(10*H*-phenothiazin-3-yl)furan-2-yl]-10*H*-phenothiazine. And that thieno[3,4-b]pyrazine contributed to the lowering of band gaps (ΔEg) than thieno[3,2-b]thiophene, thus enhancing the photoelectronic properties of the dyes. The dyes' band gaps ΔEg ranged from 1.48 to 1.88 eV; open-circuit voltage (V_{OC}) values ranged from 0.60 to 0.98 eV, and light-harvesting efficiency (LHE) values ranged from 0.6583 to 0.9444. Phenoxazin-3-yl-furan-2-yl-10*H*-phenoxazine-thieno[3,4-b][1,4]dioxine-thieno[3,4-b]pyrazine dye (PODB), phenoxazin-3-yl-furan-2-yl-10*H*-phenoxazine-thieno[3,4-b][1,4]dthiine-thieno[3,4-b]pyrazine dye (POTB), and phenothiazin-3-yl-furan-2-yl-10*H*-phenothiazine-thieno[3,4-b]dioxine-thieno[3,2-b]thiophene dye (PZDT) were identified as the most suitable candidates for DSSC applications based on molecular, optical, and most photovoltaic parameters.

Keywords: Phenothiazine-based, Optoelectronic properties, NLO, DSSC

INTRODUCTION

The use of renewable resources, such as solar energy, has been made possible by several technologies to mitigate the environmental problems and scarcity associated with fossil fuels. Many techno-industries have worked extremely hard to develop cutting-edge sustainable energy technology that is both dependable and affordable [1]. Solar energy is a renewable energy source that uses solar cells to transform sunlight into electricity. Compared to other energy sources, it offers various advantages, such as not producing greenhouse gases or nuclear waste [2]. It is predicted that solar cells of 10 % power, constructed on just 0.1% of the earth's surface, will be sufficient to meet current technological and industrial energy needs. An effective strategy to increase the formation of photocurrents and, consequently, the photo-voltaic efficiency of DSSCs appeared to be the invention of novel dyes that properly complement the solar emission spectrum [1-3].

A dye-sensitized solar cell (DSSC) uses a dye-sensitizer to absorb sunlight and generate an electric current [4]. The performance of a DSSC depends on the choice of dye. DSSCs

*Corresponding author. E-mail: bsemire@lautech.edu.ng

are cost-effective and easy to manufacture, making them attractive for replacing non-renewable energy sources and reducing environmental pollution [5-8]. DSSCs function by incorporating components such as dye sensitizers, mesoporous semiconductors (perhaps a metal oxide-like), electrolytes, counter electrodes, and photoelectrodes. Therefore, a typical DSSC consists of four basic parts: the photoanode, the cathode, the electrolyte, and the sensitizer [6]. The engineering design of DSSCs is based on employing photosensitive materials in solar cells which consist of a thin layer of nanocrystalline metal oxide, such as zinc oxide (ZnO) or titanium dioxide (TiO_2), is placed on a glass substrate to form the photoanode of a DSSC. The sensitizers, whether synthetic or natural, are essential parts of DSSCs and are crucial in broadening their absorption spectra. Different natural, organic, and organometallic dyes can be used as sensitizers in this way. The I^-/I_3^- (iodide/triiodide) redox couple, which is closed by a counter-electrode commonly made of platinum (cathode), makes up the electrolyte of a DSSC [8,9].

Several organic dye sensitizers have been examined as electron donor units and used in DSSCs, including triphenylamine, coumarin, carbazole [10], phenothiazine, indoline, porphyrin, tetrahydroquinoline [11], and metal-based donors or sensitizers such as ruthenium based complexes [12,13], Co(II/III) based dyes [14,15] and Cu based dyes [16,17]. Conversely, these metal dye-sensitizers have been reported to have exhibited about 13% to 15% in solar energy conversion efficiency [13-17]. On the other hand, cyano acrylic acid has been a preferred anchoring acceptor (A) unit due to its electron-withdrawing, as well as its ability to bond very well to semiconductor surfaces [18]. The choice of π-bridge is regarded as the most important component, even though donor and acceptor building blocks are essential for producing highly effective D-π-A dyes [19]. The planarity of π-bridges with both donor and acceptor is very essential to effectively inhibit unwanted charge recombination during intra-molecular electron transfer [20,21]. Also, in order to achieve this, other potential structures of artificial sensitizers, including D-A-π-A [22], D-D-π-A [23], D-π-A-A, D-A-A [24] and A-π-D-π-A [9] are well-known and gained significant importance due to their high efficacy.

Density functional theory (DFT) approaches are useful for describing ground state properties of molecules and deliver reliable results when analyzing the electrical properties of many-electron systems [24-26]. Thus, DFT and Time-Dependent DFT (TD-DFT) have been widely employed in the study of molecular, electrical, and photoelectric properties of either isolated, polymeric, and condensed molecules [27], as well as for estimation of photoelectric properties of dye-sensitizers for DSSCs [28-30].

Phenothiazine (PTZ), a well-known donor, has sulfur and nitrogen that are rich in electrons. Its ring is non-planar and has a butterfly conformation in the ground state, which can stop molecules from aggregating and lead to the production of molecular excimer [10,30,31]. Phenothiazine-based dyes' aggregation behavior has been investigated [32]. Due to the additional electron-rich sulfur atom, PTZ is a better donor than other amines like triphenylamine, tetrahydroquinoline, carbazole, and iminodibenzyl, and those containing different -spacers have been thoroughly investigated [10,33-35].

Phenothiazine-based dyes coupled with other electron-donating groups, such as triphenylamine have been explored, but the results showed poor efficiency of the studied dyes [36,37]. Also, phenothiazine (PTZ) and phenoxazine (POZ) donor moieties have distinctive electrical and optical characteristics that are considered capable of pushing electrons in organic dye sensitizers for application in DSSCs. The synthesized dimer of PTZ and POZ chromophores coupled with different donor moieties achieved the power conversion efficiency (PCE) of 5.87 and 6.40 % [38], 5.40 [39], 3.78, 4.41, 2.48 [36], and 6.6, 7.8, 7.1, 6.55 % [40] conversion efficiencies. Recently, a series of 2-[3-(10H-phenothiazin-3-yl)furan-2-yl]-10H-phenothiazine (JK-POZ, 1-3) and 2-[3-(10H-phenoxazin-3-yl)furan-2-yl]-10H-phenoxazine (JK-PTZ, 1-3) dyes were designed in form of D–π–A–A organic dyes. The results showed that JK-POZ-3 and JK-PTZ-3 dyes (i.e., 2-[3-(10H-phenothiazin-3-yl)furan-2-yl]-10H-phenothiazine and 2-[3-(10Hphenoxazin-3-yl)furan-2-yl]-10H-phenoxazine dyes containing 3,4-ethylenedioxythiophene - bisthieno[3,2-b:2',3'-d]thiophene π-linker showed outstanding optoelectronic properties [41]. In extension of this work, two series of dyes were designed by changing 3,4-ethylenedioxythiophene π-linker to 1,3-dihydro-2,1,3-benzothiadiazole, and thienothiophene π-linker to bisthieno[3,2-b:2',3'-d]thiophene as reported [42].

The results revealed that the HOMO energy, E_{LUMO}-E_{HOMO} energy, injection drive force, reorganization energy (λ_{total}) and coupling constant ($|VRP|$) favored dyes with 3,4-ethylenedioxythiophene (PBPD dyes) over 1,3-dihydro-2,1,3-benzothiadiazole (PTPD dyes) [42].

In furtherance of the study of the effects of π-linkers on the molecular, electronic, and photoelectrical properties of phenothiazine and phenoxazine-based dye-sensitizers [41,42], this work was designed in such that 2,3-dihydrothieno[3,4-b][1,4]dioxine/thieno[3,4-b][1,4]dithiine and thieno[3,2-b]thiophene/thieno[3,4-b]pyrazine π-linkers were used to give eight unique dyes as shown in Fig. 1. The dyes with 2-[3-(10H-phenoxazin-3-yl)furan-2-yl]-10H-phenoxazine and 2-[3-(10H-phenothiazin-3-yl)furan-2-yl]-10H-phenothiazine as donor units are denoted with prefix PO and PZ, respectively.

COMPUTATIONAL DETAILS

The graphic user interface of Spartan 14, a quantum chemical software package was used for the optimization of the designed sensitizers. The geometrical optimization of the designed D-π-A dyes was carried out at DFT of the three-parameter density functional (B3LYP), which includes the Lee, Yang, and Parr correlation functional and Becke's gradient exchange correction with 6-31G** basis set. To ascertain the local minimum on the potential energy surface, frequency calculations at the same theoretical level were performed on the geometry. Also, TD-DFT was performed on the dyes for ultraviolet-visible (UV-Vis) absorption spectra calculations, this method has been described as good enough to be adequate and productive for estimating the excitation properties of organic dyes [43-45].

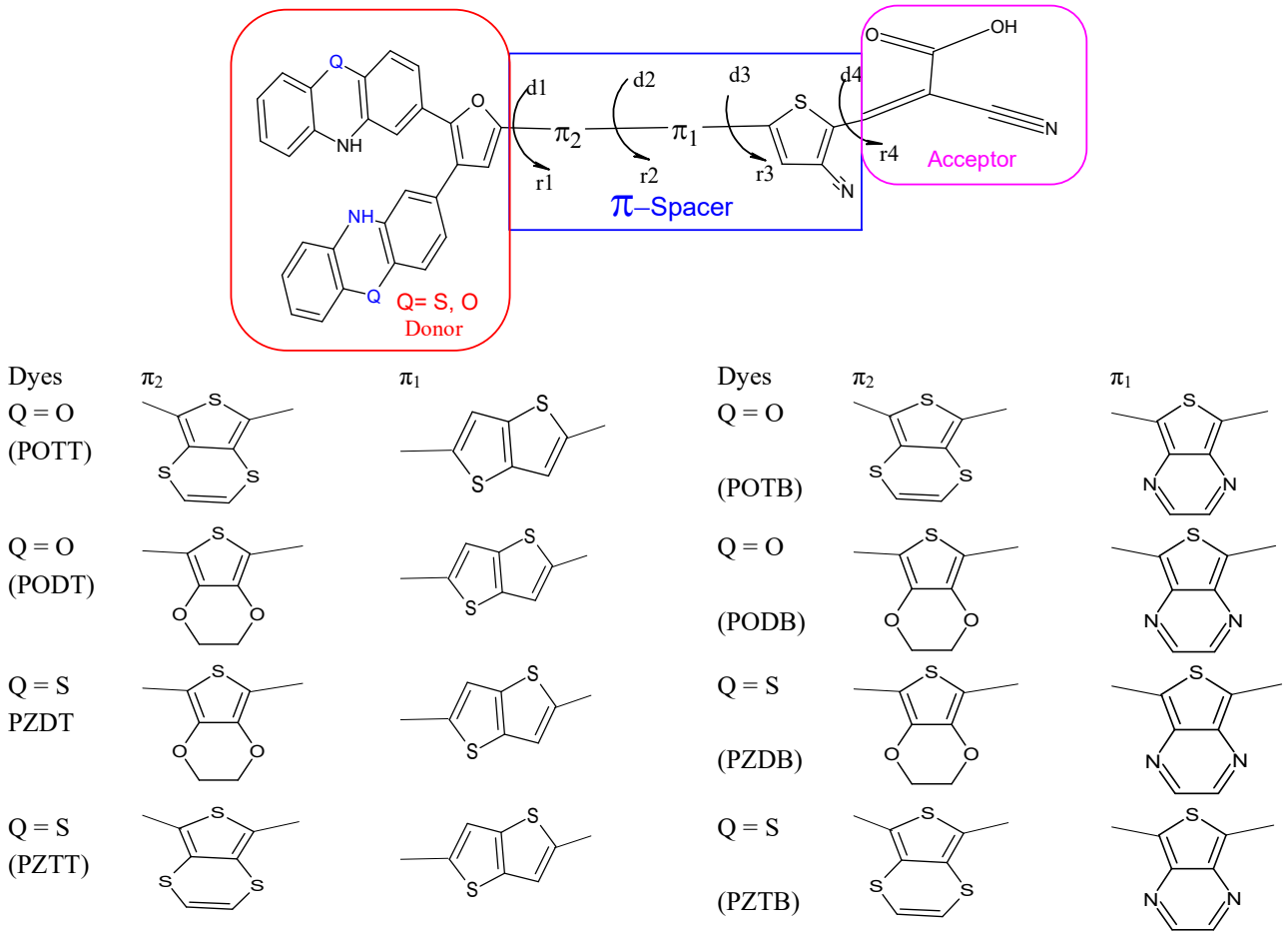

Fig. 1. Schematic structure of the simulated dyes with the conjugated π-linkers.

The frontier orbitals energy (the HOMO and LUMO) levels were calculated to provide easy access to the molecular descriptors, the conceptual DFT method was used to determine the chemical reactivity parameters such as chemical hardness (η), global electrophilicity index (ω), electro-donating power (ω^+) and electro-accepting power (ω^-) as described in [46] as shown in Eqs. (1)-(4):

$$\eta = \frac{(IP - EA)}{2} \tag{1}$$

$$\omega = \frac{(IP + EA)^2}{4(IP - EA)} \tag{2}$$

$$\omega^+ = \frac{(IP + 3EA)^2}{16(IP - EA)} \tag{3}$$

$$\omega^- = \frac{(3IP + EA)^2}{16(IP - EA)} \tag{4}$$

where ionization potential (IP) and electron affinity (EA) are approximated to be negative of the HOMO ($IP = -E_{HOMO}$) and LUMO ($EA = -E_{LUMO}$), respectively [47].

The short-circuit current density (J_{SC}) and the open-circuit photo-voltage (V_{OC}) are the two primary factors that affect the power conversion efficiency (PCE) of solar cells as shown in Eq. (5) [41,48].

$$PCE = \frac{J_{SC}V_{OC}}{P_{in}} FF \tag{5}$$

where P_{in} is the incident solar power on the cell and *FF* is the fill factor. J_{SC} in the equation 5 is calculated using Eq. (6) [49,50]:

$$J_{SC} = q \int LHE(\lambda)\, \phi_{inj} \eta_{coll} d\lambda \tag{6}$$

where LHE (λ) signifies the light-harvesting efficiency at a specific wavelength, q is the charge of the electron, ϕ_{inj} represents the electron injection efficiency, and η_{coll} indicates the charge-collection efficiency.

However, LHE plays a great role in determining J_{SC} and performance of DSSCs. A large LHE is often associated with a large photocurrent, and it is calculated using Eq. (7) [51]:

$$LHE = 1 - 10^{-f} \tag{7}$$

where f is the oscillator strength corresponding to the maximum wavelength (λ_{max}) of the dye.

Furthermore, other parameters that are essential for the performance of DSSC are the free energy of electron injection (ΔG_{inject}) and the driving force regeneration (ΔG_{reg}). The ΔG_{inject} can be computed using Eq. (8) [52].

$$\Delta G_{inject} = E^{dye^{**}} - E_{CB} \tag{8}$$

where E_{CB} is the reduction potential of the TiO_2 conduction band, CB (-4.0 eV) and $E^{dye^{**}}$ is the oxidation potential energy of the dye in the excited state [53] as shown in Eq. (9)

$$E^{dye^{**}} = E^{dye} - E^{oo} \tag{9}$$

And where $E^{dye^{**}}$ is the oxidation potential energy of the dye in the excited state, E^{oo} stands for the vertical transition energy corresponding to the λ_{max} and E^{dye} indicates the oxidation potential of the molecule in the neutral state ($E^{dye} = -E_{HOMO}$) [54].

The ΔG_{reg} on the other hand, is determined using Eq. (10):

$$\Delta G_{reg} = E^{dye} - E_{I^-/I_3^-} \tag{10}$$

where E_{I^-/I_3^-} is the redox potential energy of the redox electrolyte -4.70 eV [18].

The theoretical open-circuit voltage (V_{OC}), an essential parameter to measure the force that drives electrons and subsequently photoelectric current is calculated as ($V_{OC} = E_{LUMO} - E_{CB}$), and the V_{OC} increases as the E_{LUMO} increases [55]. The total energy of the rearrangement of dyes ($\lambda_{total} = \lambda_h + \lambda_e$) is determined from the optimized energies of the positive and negative states of the dyes [9]. The hole (λ_h) and electron (λ_e) reorganization energies are estimated using Eqs. (11) and (12). And they have a significant effect on J_{SC}, high LHE value is known to require a small total reorganization energy [56,57].

$$\lambda_h = (E_0^+ - E_+^+) + (E_+^0 - E_0) \tag{11}$$

$$\lambda_e = (E_0^- - E_-^-) + (E_-^0 - E_0) \tag{12}$$

where E_0, E_0^+ (E_0^-), $E_+^+(E_-^-)$ and $E_+^0(E_-^0)$ stand for the optimized energy of the neutral molecule, the energy of the cation (anion) based on the neutral molecule geometry, the energy of the optimized cation (anion) structures, and the energy of the neutral molecule calculated at the cationic (anionic) state.

RESULTS AND DISCUSSION

The Backbone Geometries of the Dyes

The geometric optimization of the dye-sensitizers was carried out in the ground state in vacuum with the B3LYP/6-31G** level of theory. The optimized structures and the backbone/selected geometries are displayed in Fig. 2 and Table 1, respectively. The geometrical parameters are the bond distance (r) and dihedral angles (d) as shown in Fig. 1, where d1 (r1), d2 (r2), d3 (r3) and d4 (r4) represent the dihedral angle (bond distance) of D-π2, π2-π1, π1-cyanothiophene and 3-cyanothiophene-anchoring group, respectively. It has been reported that planarity and steric hindrance affect the molecular stability and mobility of π-electrons; hence the intramolecular charge transfer (ICT) and performance of the dye [58].

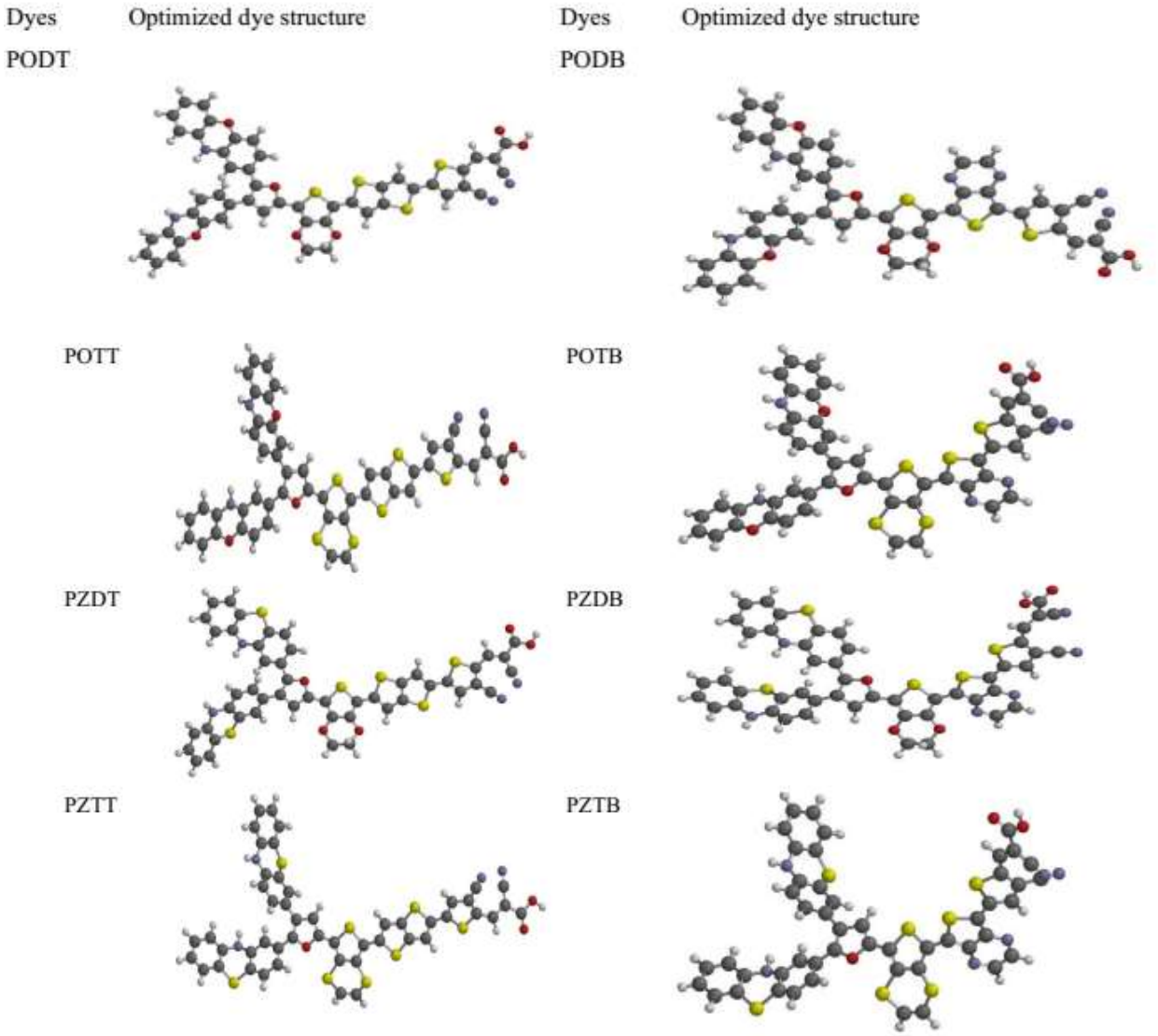

Fig. 2. Structural optimization of the studied molecules.

Table 1. Distances of r (Å) and the Dihedral Angles d (°) of the Studied Dyes

Dyes	d1 (°)	r1 (Å)	d2 (°)	r2 (Å)	d3 (°)	r3 (Å)	d4 (°)	r4 (Å)
POTT	162.31	1.437	166.30	1.446	165.35	1.440	-147.68	1.436
PZTT	-178.52	1.430	-168.86	1.436	-165.09	1.438	148.32	1.434
PODT	-162.89	1.437	-164.58	1.446	-165.02	1.440	147.66	1.436
PZDT	-178.15	1.430	-168.59	1.436	-164.82	1.438	148.12	1.434
POTB	-164.41	1.438	-129.15	1.447	-178.00	1.438	148.69	1.435
PZTB	-177.98	1.429	-143.40	1.432	174.85	1.434	-147.85	1.435
PODB	-170.01	1.437	-130.63	1.445	-178.27	1.437	148.74	1.435
PZDB	-178.20	1.427	-178.09	1.419	-176.35	1.430	150.80	1.430

To facilitate intramolecular charge transfer and bathochromic shift of a dye-sensitizer, a smaller torsion angle or co-planarity of the dye is preferable [59]. The effects of π-linkers on the geometries of the dyes could be analyzed by first considering phenoxazin-3-yl-furan-2-yl-10*H*-phenoxazine-thieno[3,4-b][1,4]dthiine-thieno[3,2-b] thiophene dye (POTT) and phenoxazin-3-yl-furan-2-yl-10*H*-phenoxazine-thieno[3,4-b][1,4]dioxine-thieno[3,2-b] thiophene dye (PODT) or phenothiazin-3-yl-furan-2-yl-10*H*-phenothiazine-thieno[3,4-b][1,4]dthiine-thieno[3,2-b] thiophene dye (PZTT) and phenothiazin-3-yl-furan-2-yl-10*H*-phenothiazine-thieno[3,4-b][1,4]dioxine-thieno[3,2-b] thiophene dye (PZDT). The backbone geometries of POTT (PZTT) and PODT (PZDT) dyes (i.e. by changing π2-linker from 2,3-dihydrothieno(3,4-b)[1,4]dioxine to thieno[3,4-b] dithiine) shows that phenoxazin-3-yl-furan-2-yl-10*H*-phenoxazine-thieno[3,4-b][1,4]dthiine-thieno[3,2-b] thiophene (POTT) and phenoxazin-3-yl-furan-2-yl-10*H*-phenoxazine-thieno[3,4-b][1,4]dioxine-thieno[3,2-b]thiophene (PODT) or phenothiazin-3-yl-furan-2-yl-10*H*-phenothiazine-thieno[3,4-b][1,4]dthiine-thieno[3,2-b] thiophene (PZTT) and phenothiazin-3-yl-furan-2-yl-10*H*-phenothiazine-thieno[3,4-b][1,4]dioxine-thieno[3,2-b] thiophene (PZDT) have very similar geometries and hence may have a little or no appreciable effect on ICT of these dyes. However, considering POTT (PZTT) and phenoxazin-3-yl-furan-2-yl-10*H*-phenoxazine-thieno[3,4-b][1,4]dthiine-thieno[3,4-b]pyrazine (POTB) phenothiazin-3-yl-furan-2-yl-10*H*-phenothiazine-thieno[3,4-b][1,4]dthiine-thieno[3,4-b]pyrazine (PZTB) or PODT (PZDT) and Phenoxazin-3-yl-furan-2-yl-10*H*-phenoxazine-thieno[3,4-b][1,4]dioxine-thieno[3,4-b]pyrazine (PODB) phenothiazin-3-yl-furan-2-yl-10*H*-phenothiazine-thieno[3,4-b][1,4]dioxine-thieno[3,4-b] pyrazine (PZDB) dyes (i.e. by changing π1-linker from thieno[3,2-b]thiophene to thieno[3,4-b]pyrazine) indicates that d2 (r2) and d3 (r3) geometries of the dyes are affected (Table 1). For instance, d2 (r2) and d3 (r3) are -164.58° (1,446 Å) and -165.02° (1,440 Å), respectively for PODT, whereas they are 130.00° (1.445 Å) and -178.23° (1,437 Å) of PODB, respectively. Likewise, the d2 (r2) and d3 (r3) for POTT are 166.30° (1.446 Å) and 165.35° (1.440 Å), but they are -129.15° (1.447 Å) and -178.00° (1.438 Å) for POTB, respectively (Table 1). This shows that the intra-charge transfers and photoelectronic current are expected to be affected by changing thieno[3,2-b]thiophene to thieno[3,4-b]pyrazine in the dye [60,61]. Also, 2-[3-(10H-phenothiazin-3-yl)furan-2-yl]-10H-phenothiazine (PZ) dye series are generally more planar around d1 and d2 than 2-[3-(10H-phenoxazin-3-yl)furan-2-yl]-10H-phenoxazine (PO) dye series which may possibly lead to effective intramolecular charge transfer and conjugation than corresponding PO dyes, thus shorten of r1 and r2 bond lengths (Table 1).

Frontier Molecular Orbitals

Frontier molecular orbitals (the HOMO and LUMO) are essential parameters that provide detailed optoelectronic characteristics of a dye [9,62]. These orbitals can be used to analyze charge density distributions and charge stability, as well as the nature of electronic transitions in a dye from the ground state (the HOMO) to the excited state (the LUMO) [9,63]. The frontier orbitals overlaid presented in Fig. 3 show that the HOMOs overlaid are on the donor unit and the

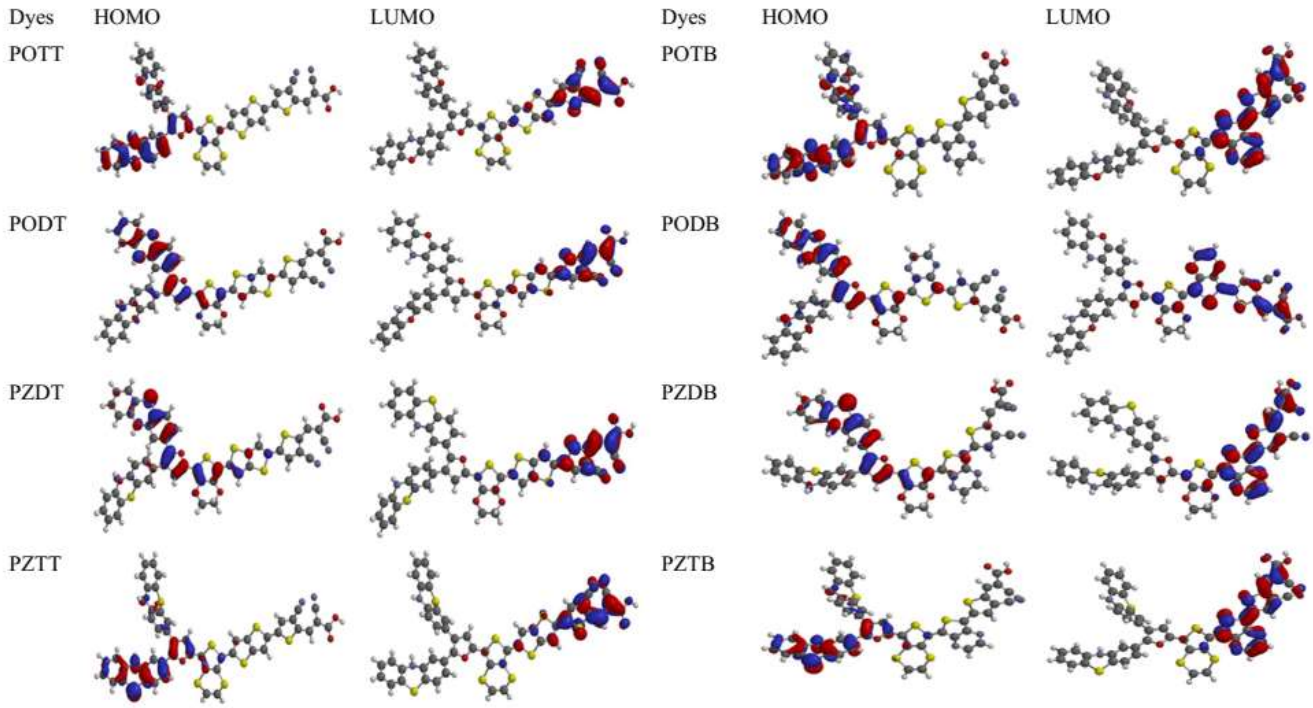

Fig. 3. Frontier molecular orbitals overlaid contours of the dyes.

LUMOs overlaid are towards the acceptor unit, this is an indication of a possible transfer of charges from the donor unit through π-linker to the anchoring unit in a pull-push manner [64,65]. The HOMO-LUMO band gap (E_g) shows the effect of π-spacers/linkers on the electrical and optoelectronic properties of a dye with small band gap favors or facilitates strong charge transfer and vice versa [41,66,67].

The operational theory of DSSC devices requires that photosensitizer materials should have the appropriate energy levels for electron injection and material regeneration to be possible. Therefore, Fig. 4 shows that the HOMO energies of all dyes are lower than the redox potential of I^-/I_3^- (-4.70 eV) which is critical for dye regeneration, and the LUMO energies are well above -4.00 eV of the conduction band (CB) of the TiO_2, suggesting that the electrons can be injected into the semiconductor quickly during the molecules' excitation [18]. The HOMO energy values of the dyes are ordered as PODT (-4.72 eV) > PODB (-4.76 eV) > POTT (-4.83 eV) > POTB (-4.84 eV) > PZDT (-4.89 eV) > PZDB (-4.95 eV) > PZTT (-5.04 eV) > PZTB (-5.06 eV), indicating that PZTB, PZTT, PZDB, and PZDT dyes have higher regeneration capacities. Meanwhile, the LUMO energies are -3.14 (POTT), -3.16 (PZTT), -3.05 (PZDT), -3.02 (PODT), -3.40 (PZTB), -3.36 (POTB), -3.16 (PODB) and -3.22 eV (PZDB), showing that all the dyes are expected to have good drive force for electrons injection [68]. The computed energy gaps of the modeled dyes decrease in the following order: PZTT (1.88 eV) > PZDT (1.84 eV) > PZDB (1.73 eV) > PODT (1.70 eV) > POTT (1.69 eV) > PZTB (1.66 eV) > PODB (1.60 eV) > POTB (1.48 eV). This shows that 2-[3-(10H-phenoxazin-3-yl)furan-2-yl]-10H-phenoxazine (PO) dyes generally have lower Eg than 2-[3-(10H-phenothiazin-3-yl)furan-2-yl]-10H-phenothiazine (PZ) dyes, indicating 2-[3-(10H-phenoxazin-3-yl)furan-2-yl]-10H-phenoxazine has strong electron donating ability that 2-[3-(10H-phenothiazin-3-yl)furan-2-yl]-10H-phenothiazine which agreed with earlier observation [41]. Likewise, changing the π1-linker from thieno[3,2-b]thiophene to thieno[3,4-b]pyrazine lowers the Eg, which should enhance photoelectronic properties in line with observed geometries [58]. It is also suggested that PZTB, PODB, and POTB should have better short-circuit current density (J_{SC}) and thus, viable dye-sensitizer candidates for DSSC application (Fig. 4).

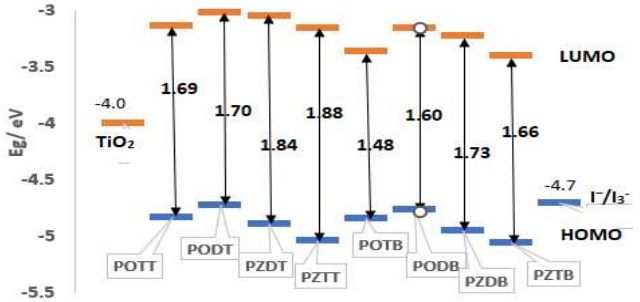

Fig. 4. The frontier orbital energy Gap of the dyes.

Natural Bond Orbital (NBO) Analysis

The primary goal of population analysis in D-π-A structures is to provide a picture of the charge distribution and electron transfer from a subsystem's filled Donor (D) orbital to another subsystem's vacant acceptor (A) orbital. [23,69]. NBO population analysis was carried out based on the optimized geometries of the ground state to analyze the charge population of the dyes. Table 2 shows the computed NBO values of D, π-linker, A, and D-A at the B3LYP/6-31G** level. The positive values of NBO charges are present on the donor moiety of the dyes, indicating that they can function as an efficient electron-donor group. On the other hand, the negative NBO values on acceptor groups indicated that they are effective electron-withdrawing groups [58]. The charges on π-conjugated linkers are very small and tend towards zero, indicating that they might not trap the electrons and serve as a transporter for the mechanism that transfers electrons from D to A units. The NBO charges on the donor groups of each molecule are organized as follows during photoexcitation: PODB (0.141e) > PZDB (0.124e) > PODT (0.116e) > POTB (0.108e) > POTT (0.107e) > PZDT (0.106e) > PZTB (0.093e) > PZTT (0.092e), indicating that PODB, PZDB and PODT have higher NBO charge density values (Table 2). Additionally, q(D-A) denotes the distinction between the electron acceptor and donor. PODB has the highest q(D-A) (0.276e), followed by PZDB (0.235e), PODT (0.221e), PZDT (0.209e), POTB (0.204e), POTT (0.199e), PZTB (0.186e) and PZTT (0.182e), indicating that these dyes have bigger charge separation than the other dyes. Also, dyes with thieno[3,4-b]pyrazine as π-linker (π1) have a larger intramolecular charge separation state between the D and A units. Thus, an effective intramolecular charge separation state between the D and A units can lead to efficient electron transfer and, ultimately, an electron injection into the conduction band of TiO_2 [41]. Also, dyes with 2,3-dihydrothieno[3,4-b][1,4]dioxine as π2-linker (*i.e.* PODB, PODT, PZDB, and PZDT) show large intramolecular charge separation, which will improve electron injection driving force.

Table 2. The Natural Bond orbital Charge (e) of the Fragments of Dyes in the Ground State at the B3LYP/6-31G** Level of Theory

Dyes	Donor	π-Spacer	Acceptor	q(D-A)
POTT	0.107	-0.014	-0.092	0.199
PZTT	0.092	-0.006	-0.090	0.182
PODT	0.116	-0.014	-0.105	0.221
PZDT	0.106	-0.001	-0.103	0.209
POTB	0.108	-0.012	-0.096	0.204
PZTB	0.093	0.000	-0.093	0.186
PODB	0.141	-0.016	-0.135	0.276
PZDB	0.124	-0.014	-0.111	0.235

MEP maps are one of the parameters that provide details on the interactions between molecules that form hydrogen bonds and their reactive sites [58]. Also, it helps in estimating the forms, sizes, charge densities, and delocalization of systems as well as the charge distributions on those systems in three dimensions [58]. As shown in Fig. 5, the simulated MEP maps exhibit three different colors: from red, orange, green to blue. The negative electrostatic potential or high electron density area is represented by red or yellow, the positive electrostatic potential or low electron density area is represented by blue, and the intermediate region is shown by green [70,71]. The blue region of the dyes shows acidic hydrogen atoms or electrophilic centers, while the red region is primarily found around oxygen atoms and cyano groups or nucleophilic centers. An area with no electrostatic potential or a neutral region is indicated by green [58]. The blue color of the hydroxyl hydrogen atom shows that it is very acidic and can be readily given out, and the red color is on the carbonyl oxygen of the carboxylic group, indicating that all the designed dyes have a high possibility of effective coupling/anchoring with TiO_2. The red color on the cyano group near the carboxylic group and cyano-thiophene as a result of high electron density makes the area the most profitable site for the electrolyte [9].

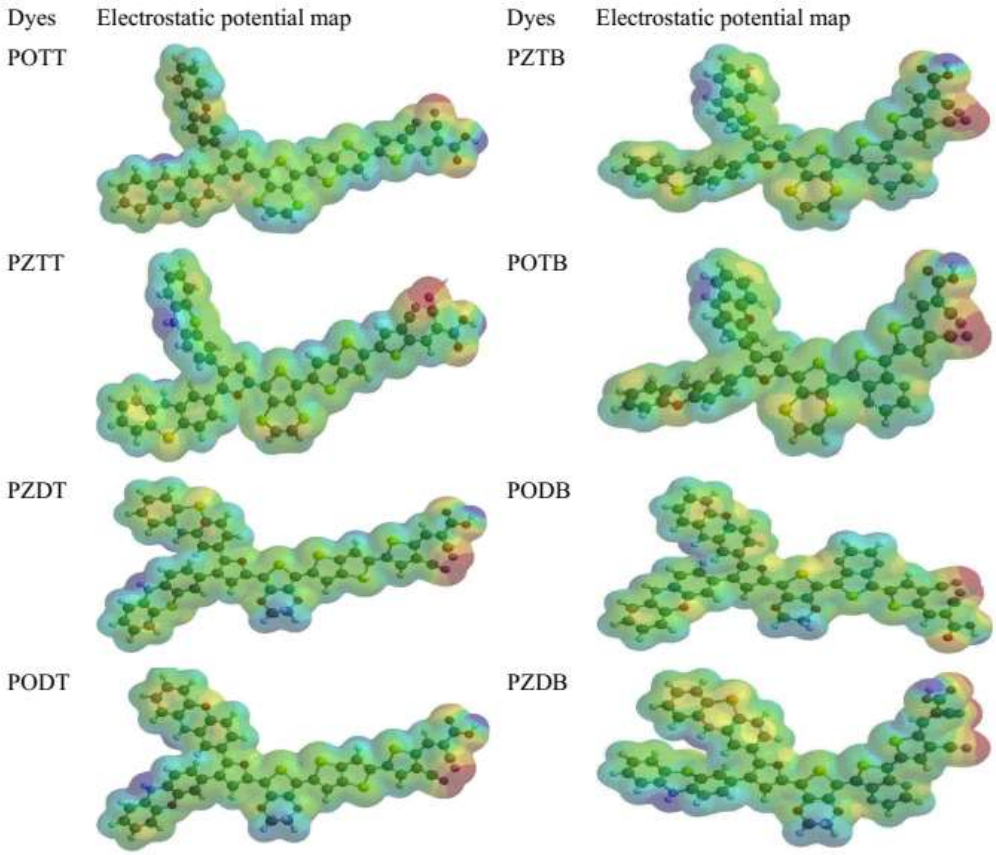

Fig. 5. Molecular electrostatic potential maps for the simulated dyes.

Table 3. Chemical Parameters and the Calculated Reactivity Indices of the Dye-Sensitizers Calculated at DFT/6-31G** Level

Dyes	IP (eV)	EA (eV)	η (eV)	ω^+ (eV)	ω^- (eV)	ω (eV)
POTT	4.83	3.14	0.85	9.40	7.51	11.49
PZTT	5.04	3.16	0.94	8.94	7.01	11.11
PODT	4.72	3.02	0.85	8.81	6.98	10.85
PZDT	4.89	3.05	0.92	8.57	6.70	10.67
POTB	4.84	3.36	0.74	11.36	9.40	13.50
PZTB	5.06	3.40	0.83	10.78	8.77	13.00
PODB	4.76	3.16	0.80	9.80	7.92	11.88
PZDB	4.95	3.22	0.87	9.65	7.71	11.80

Quantum Chemical Reactivity Indicators

The ionization potential (IP), electron affinity (EA), chemical hardness (η), electrophilicity index (ω), electron-donating power (ω^-), and electron-accepting power (ω^+) are some of the essential chemical reactivity indicators calculated and listed in Table 3. The IP is associated with the energy shift that occurs when a molecule adds holes or extracts electrons, whereas EA is the energy change that occurs when a molecule absorbs electrons or extracts holes. A dye-sensitizer performs two functions in DSSCs by injecting an excited electron into TiO_2 and pulling an electron from the electrolyte to fill the hole; thus, information on gaining and losing electrons or holes in a dye is related to the magnitude of electron affinity and ionization potential of the

dye [72]. The IP and EA values favor PODT and PODB (Table 3). The chemical hardness (η) has been attributed to the easiness of intramolecular charge transfer in a dye and its low value to promote charge transfer and separation [73]. The η values are ordered as PZTT > PZDT > PZDB > PODT > POTT > PZTB > PODB > POTB, indicating that POTB, PODB, and PZTB dyes have the lowest chemical hardness, and thus, should be able to transfer electrons readily which may improve light to energy conversion efficiency in DSSC [74]. The value of ω can be used to evaluate the stabilization energy, while ω^+ indicates electron-accepting ability of a molecular structure; hence higher values of ω and ω^+ are preferable for a good dye-sensitizer [49]. Therefore, ω and ω^+ are ordered as: POTB > PZTB > PODB > PZDB > POTT > PZTT > PODT > PZDT, signifying that POTB, PZTB and PODB are preferred for electron-accepting power and stabilization energy abilities. The electron-donating powers (ω^-) exhibits a similar trend of electrophilicity and electron-accepting power. As a result, POTB, PZTB, and PODB dyes should have the highest short-circuit current density and the best power conversion efficiency (PCE).

Photo-absorption Properties

TD-DFT is very popular for calculating electronic transitions and ultraviolet-visible absorption spectra, so, the absorption wavelengths, oscillator strengths, and molecular orbital contributions to the electronic transitions are calculated using the TD-DFT/B3LYP/6-31G** level of theory, as shown in Table 4. The absorption λ_{max} (oscillator strength, *f*) is 596.66 (0.869), 582.76 (0.794), 489.24 (1.026), 611.98 (0.791), 640.06 (0.446), 652.20 (0.488), 635.32 (1.255) and 625.84 nm (0.614) for POTT, PZTT, PZDT, PODT, PZTB, POTB, PODB, and PZDT, respectively. This suggests that all designed dyes have strong absorption in the UV-visible region of the electromagnetic spectrum, which is very vital for photocurrent conversion in DSSC [75]. The longest wavelength for all the dyes arise from electrons transiting from H→L, which represents π→π* transitions. Also, it is noticed that 2-[3-(10H-phenoxazin-3-yl)furan-2-yl]-10H-phenoxazine (PO) dyes have longer wavelengths than 2-[3-(10H-phenothiazin-3-yl)furan-2-yl]-10H-phenothiazine (PZ) dyes, which means 2-[3-(10H-phenoxazin-3-yl)furan-2-yl]-10H-phenoxazine enhances photoelectronic properties of the dyes than 2-[3-(10H-phenothiazin-3-yl)furan-2-yl]-10H-phenothiazine. Similarly, replacement of thieno[3,2-b]thiophene with thieno[3,4-b]pyrazine also enhances the absorption properties which, in turn, adds to the improvement of photon harvesting capabilities of the dyes in line with observed geometries and frontier orbitals energies [58,65]. Therefore, PZTB, PODB, and POTB should be viable dye-sensitizer candidates for DSSC application.

Photovoltaic Parameters for DSSC Performance

The essential parameters for proper investigations of photovoltaic properties of the designed dyes such as the electron injection drive force (ΔG^{inject}), dye regeneration force (ΔG^{regen}), light harvesting efficiency (LHE), the excited-state lifespan (τ), and the reorganization energy (λ_{total}) are estimated in order to measure the J_{SC} and V_{OC}, two vital factors that determine the efficiency of PCE. The J_{SC} determined by Eq. (5), is significantly influenced by the variables such as ΔG^{inject} and LHE. To inject photoexcited electrons into the CB of TiO_2, suitable dyes must have a sizable LHE that reflects the ability of most photons in the UV-visible region to be absorbed [9,41]. The LHE, ΔG^{inject}, ΔG^{regen}, and V_{OC} values are summarized in Table 5, where PODB (0.944) and PZDT (0.906) have highest values for LHE, followed by POTT (0.865), PZTT (0.839), PODT (0.838), PZDB (0.757), POTB (0.675), and PZTB (0.658). This indicates that PODB and PZDT dyes should exhibit higher J_{SC} values. The than thieno[3,2-b]thiophene values show that electrons can be readily injected into TiO_2. The ΔG^{inject} values in Table 5 reveal that PZTB and PODT have higher electrons injection forces than POTT, PZTT, PZTB, POTB, PODB and PZDB. The regeneration driving force (ΔG^{regen}) is additional essential variable that affects the effectiveness of the DSSCs. Low ΔG^{regen} force is necessary to achieve faster regeneration of the sensitizers [9,58]. Also, the injected electrons in the excited state should be significantly greater than 0.2 eV to provide an appreciable driving force for the electron injection process [9]. The computed ΔG^{regen} values for the dyes are as follows: PZTB (0.36) > PZTT (0.34) > PZDB (0.25) > PZDT (0.19) > POTB (0.14) > POTT (0.13) > PODB (0.06) > PODT (0.02), indicating that only PZTB, PZTT and PZDB may have considerable higher driving force for regeneration. Also, the PZ dyes presented higher Voc and better ΔG^{regen} than PO dyes (Table 5).

Table 4. Absorption Wavelengths with Molecular Orbitals Involve Electronic Transitions Calculated at the TD-DFT/B3LYP/6-31G** Level

Dyes	λ_{max} (nm)	E_{ex} (eV)	f	MO involved in transitions	LHE
POTT	522.92	2.37	0.012	HOMO-3 → LUMO; 67%	
				HOMO → LUMO+1; 26%	
	528.50	2.35	0.477	HOMO → LUMO+1; 70%	
				HOMO-3 → LUMO; 28%	
	596.66	2.08	0.869	HOMO-2 → LUMO; 97%	0.8649
	808.21	1.53	0.202	HOMO → LUMO; 100%	
PZTT	455.32	2.72	0.005	HOMO-1 → LUMO+1; 98%	
	494.51	2.51	0.459	HOMO → LUMO+1; 93%	
	522.36	2.37	0.200	HOMO-3 → LUMO; 95%	
	582.76	2.13	0.794	HOMO-2 → LUMO; 97%	0.8393
	639.60	1.94	0.003	HOMO-1 → LUMO; 99%	
	723.33	1.71	0.281	HOMO → LUMO; 99%	
PZDT	435.89	2.84	0.016	HOMO-1 → LUMO+1; 80%	
	449.28	2.76	0.333	HOMO-3 → LUMO; 72%	
	489.24	2.53	1.026	HOMO → LUMO+1; 82%	0.9058
	589.76	2.10	0.551	HOMO-2 → LUMO; 97%	
	614.14	2.02	0.099	HOMO-1 → LUMO; 98%	
	730.67	1.69	0.574	HOMO → LUMO; 98%	
PODT	453.45	2.73	0.635	HOMO-3 → LUMO; 76%	
	460.74	2.69	0.008	HOMO-1 → LUMO+1; 97%	
	511.14	2.43	0.702	HOMO → LUMO+1; 90%	
	611.98	2.03	0.791	HOMO-2 → LUMO; 97%	0.8383
	671.88	1.85	0.009	HOMO-1 → LUMO; 100%	
	796.97	1.56	0.409	HOMO → LUMO; 99%	
PZTB	567.81	2.18	0.006	HOMO → LUMO+1; 96%	
	640.06	1.94	0.466	HOMO-2 → LUMO; 64%	0.6583
				HOMO-3 → LUMO; 29%	
	674.84	1.84	0.012	HOMO-3 → LUMO; 64%	
				HOMO-2 → LUMO; 32%	
	743.78	1.67	0.002	HOMO-1 → LUMO; 100%	
	858.00	1.45	0.149	HOMO → LUMO 99%	
POTB	616.43	2.01	0.013	HOMO → LUMO+1; 94%	
	652.20	1.90	0.488	HOMO-2 → LUMO; 50%	0.6747
				HOMO-3 → LUMO; 39%	
	685.17	1.81	0.049	HOMO-3 → LUMO; 53%	
				HOMO-2 → LUMO; 44%	
	842.28	1.47	0.001	HOMO-1 → LUMO; 100%	
	971.77	1.28	0.153	HOMO → LUMO; 99%	
PODB	502.27	2.47	0.002	HOMO-1 → LUMO+1; 53%	
				HOMO-2 → LUMO+1; 38%	
	510.61	2.43	0.015	HOMO-1 → LUMO+1; 46%	
				HOMO-2 → LUMO+1; 38%	
				HOMO-3 → LUMO; 12%	
	585.89	2.12	0.152	HOMO → LUMO+1; 87%	
	635.32	1.95	1.255	HOMO-2 → LUMO; 79%	0.9444
	733.35	1.69	0.013	HOMO-1 → LUMO; 96%	
	837.20	1.48	0.590	HOMO → LUMO; 90%	
PZDB	480.37	2.58	0.289	HOMO-1 → LUMO+1; 43%	
				HOMO-3 → LUMO; 41%	
	497.86	2.49	0.114	HOMO-1 → LUMO+1; 46%	
				HOMO-3 → LUMO; 34%	
	563.47	2.20	0.031	HOMO → LUMO+1; 90%	
	626.84	1.98	0.614	HOMO-2 → LUMO; 81%	0.7565
	665.06	1.86	0.158	HOMO-1 → LUMO; 83%	
	795.35	1.56	0.406	HOMO → LUMO; 96%	

Table 5. Calculated Electronic Properties of the Studied Dyes (in eV)

Dyes	λ_{max} (nm)	f	E^{oo} (eV)	E^{dye} (eV)	$E^{dye^{**}}$ (eV)	ΔG_{inject} (eV)	ΔG_{reg} (eV)	LHE	eV_{OC} (eV)
POTT	596.66	0.869	2.08	4.83	2.75	-1.25	0.13	0.865	0.86
PZTT	582.76	0.794	2.13	5.04	2.91	-1.09	0.34	0.839	0.84
PODT	611.98	0.791	2.03	4.72	2.69	-1.31	0.02	0.838	0.98
PZDT	489.24	1.026	2.53	4.89	2.36	-1.64	0.19	0.906	0.95
POTB	652.20	0.488	1.90	4.84	2.94	-1.06	0.14	0.675	0.64
PZTB	640.06	0.446	1.94	5.06	3.12	-0.88	0.36	0.658	0.60
PODB	635.32	1.255	1.95	4.76	2.81	-1.19	0.06	0.944	0.84
PZDB	625.84	0.614	1.98	4.95	2.97	-1.03	0.25	0.757	0.78

Table 6. Reorganization Energies, λ_{total} Values (eV), Coupling Constant ($|V_{RP}|$), and Electron Transfer Rate Constant (k) of the Designed Dyes

Dyes	λ_h (eV)	λ_e (eV)	λ_{total} (eV)	ΔE_{RP} (eV)	$\|V_{RP}\|$ (eV)	k × 10^{13} (s^{-1})
POTT	0.203	0.328	0.532	0.83	0.415	1.38
PZTT	0.305	0.329	0.634	1.04	0.520	46.40
PODT	0.216	0.316	0.532	0.72	0.360	4.74
PZDT	0.268	0.315	0.582	0.89	0.445	90.61
POTB	0.207	0.316	0.523	0.84	0.420	1.94
PZTB	0.338	0.322	0.660	1.06	0.530	64.90
PODB	0.216	0.316	0.532	0.76	0.380	2.84
PZDB	0.349	0.329	0.678	0.95	0.475	1.78

The efficiency of a DSSC device is also influenced by the charge-transfer rate (k) and it can be estimated from Eq. (13) [41,76].

$$k = \left(\frac{\pi}{\lambda_{total} k_B . T}\right)^{\frac{1}{2}} \frac{V^2}{\hbar} \exp\left(-\frac{\lambda_{total}}{4 k_B . T}\right) \quad (13)$$

where V is the charge-transfer coupling constant, T is the temperature, k_B is the Boltzmann constant, and the λ_{total} is the reorganization energy.

A lower value of λ_{total} should accelerate the electron transport process, thus, boosting the J_{SC}. λ_{total} is the sum of the electron-reorganization energies (λ_e) and the hole reorganization energies (λ_h). The λ_e, λ_h, λ_{total} values are shown in Table 6. The λ_{total} for the dyes increases in the following order: POTB < PODB = POTT = PODT < PZDT < PZTT < PZTB < PZDB, which suggests that PODB POTB, PODT and POTT should have good electron-transfer efficiency due to lower λ_{total} values. The charge-transfer coupling constant $|V_{RP}| = {\Delta E_{RP}}/{2}$, where ΔE_{RP} is calculated from Eq. (14).

$$\Delta E_{RP} = E_{HOMO}^{dye} - E_{CB}^{TiO_2} \quad (14)$$

The V_{RP} values in Table 6 reveal that PZTT, PZDT, and PZTB with higher V_{RP} values presented greater electron transfer rate constant (k), as is presented in Table 6, and should result in a better sensitizer [42].

CONCLUSION

DFT and TD-DFT computational techniques were used to investigate eight designed dye-sensitizers in the form of phenothiazine and phenoxazine-based D-A-π-A architecture. The effects 2,3-dihydrothieno[3,4-b][1,4]dioxine/thieno[3,4-b][1,4]dithiine and thieno[3,2-b]thiophene/thieno[3,4-b]

pyrazine as π-linkers on the molecular, optoelectronic characteristics and chemical reactivities of the dyes were investigated. The results show that:

1. All the dyes have the necessary HOMO energies for the electrolyte's redox potential (I^-/I_3^-), and their LUMO energies are also appropriate for the conduction band of the semiconductor TiO_2.
2. Generally, 2-[3-(10H-phenoxazin-3-yl)furan-2-yl]-10H-phenoxazine (PO) dyes are more planar around d1 and d2 with lower band gap energies than 2-[3-(10H-phenothiazin-3-yl)furan-2-yl]-10H-phenothiazine (PZ) dyes, which means 2-[3-(10H-phenoxazin-3-yl)furan-2-yl]-10H-phenoxazine donor unit has strong electron donating ability than 2-[3-(10H-phenothiazin-3-yl)furan-2-yl]-10H-phenothiazine donor unit, this is supported by backbone geometries, molecular reactivity indicators and optical properties. However, ΔG_{reg} and λ_{total}, $|V_{RP}|$ and k suggest that PZ dyes could possess good electron-transfer efficiency due to lower regeneration energy, higher coupling constant, and electron transfer rate constant.
3. Thieno[3,4-b]pyrazine as π-linker lowers the energy band gap, which can enhance the photoelectronic properties of the dyes than thieno[3,2-b]thiophene.
4. LHE and electron injection drive force (ΔG^{inject}) favor PODB and PZDT, while the reorganization energy (λ_{total}) favors PODB and POTB. Therefore, PODB, POTB, and PZDT dyes can be considered as the most probable candidates for DSSC application.

ACKNOWLEDGMENTS

The authors are grateful to the Departments of Chemistry, Federal University Lokoja Nigeria for providing the laboratory space and facilities used in this research work.

REFERENCES

[1] Periyasamy, K.; Sakthivel, P.; Vennila, P.; Anbarasan, P. M.; Venkatesh, G.; Sheena Mary, Y., Novel D-π-A Phenothiazine and Dibenzofuran Organic Dyes with Simple Structures for Efficient Dye-Sensitized Solar Cells. *J. Photochem. Photobiol. A Chem.* **2021**, *413* (March), 113269. https://doi.org/10.1016/j.jphotochem.2021.113269.

[2] Sharmoukh, W.; Cong, J.; Ali, B. A.; Allam, N. K.; Kloo, L., Comparison between Benzothiadizole-Thiophene-and Benzothiadizole-Furan-Based D-A-Ï€-A Dyes Applied in Dye-Sensitized Solar Cells: Experimental and Theoretical Insights. *ACS Omega* **2020**, *5* (27), 16856-16864. https://doi.org/10.1021/acsomega.0c02060.

[3] Kurumisawa, Y.; Higashino, T.; Nimura, S.; Tsuji, Y.; Iiyama, H.; Imahori, H., Renaissance of Fused Porphyrins: Substituted Methylene-Bridged Thiophene-Fused Strategy for High-Performance Dye-Sensitized Solar Cells. *J. Am. Chem. Soc.* **2019**, *141* (25), 9910-9919. https://doi.org/10.1021/jacs.9b03302.

[4] Darmawan, M. I., Studi Fabriksi Dye Sensitized Solar Cells (Dssc) Mengunakan Dye Cellosia Argentum. *Indones. Phys. Rev.* **2019**, *2* (3), 116-122. https://doi.org/10.29303/ipr.v2i3.33.

[5] Huang, Z.S.; Meier, H.; Cao, D., Phenothiazine-based dyes for efficient dye-sensitized solar cells. *J. Mater. Chem. C.* **2016**, *4* (13), 2404-2426. https://doi.org/10.1039/c5tc04418a.

[6] Abubakari, I.; Babu, S.; Vuai, S.; Makangara, J., 2-Hexylthiophene-Substituted Alizarin-Based (D-π-A) Organic Dyes for Dye-Sensitized Solar Cell Applications: Density Functional Theory and UV-Vis Studies. *J. Chem. Res.* **2021**, *45* (1-2), 13-20. https://doi.org/10.1177/1747519820922450.

[7] Zhang, M. D.; Pan, H.; Ju, X. H.; Ji, Y. J.; Qin, L.; Zheng, H. G.; Zhou, X. F., Improvement of Dye-Sensitized Solar Cells' Performance through Introducing Suitable Heterocyclic Groups to Triarylamine Dyes. *Phys. Chem. Chem. Phys.* **2012**, *14* (8), 2809-2815. https://doi.org/10.1039/c2cp23876d.

[8] Younas, M.; Baroud, T. N.; Gondal, M. A.; Dastageer, M. A.; Giannelis, E. P., Highly Efficient, Cost-Effective Counter Electrodes for Dye-Sensitized Solar Cells (DSSCs) Augmented by Highly Mesoporous Carbons. *J. Power Sources* **2020**, *468*, 228359. https://doi.org/10.1016/j.jpowsour.2020.228359.

[9] Azaid, A.; Raftani, M.; Alaqarbeh, M.; Kacimi, R.; Abram, T.; Khaddam, Y.; Nebbach, D.; Sbai, A.; Lakhlifi, T.; Bouachrine, M., New Organic Dye-Sensitized Solar Cells Based on the D-A-π-A Structure for Efficient DSSCs: DFT/TD-DFT Investigations. *RSC Adv.* **2022**, *12* (47), 30626-30638.

https://doi.org/10.1039/d2ra05297k.

[10] Ouared, I.; Rekis, M.; Trari, M., Phenothiazine Based Organic Dyes for Dye Sensitized Solar Cells: A Theoretical Study on the Role of π-Spacer. *Dye. Pigment.* **2021**, *190*, 109330. https://doi.org/10.1016/j.dyepig.2021.109330.

[11] Wang, T.; Hao, X.; Han, L.; Li, Y.; Ye, Q.; Cui, Y., D-A-π-A Carbazole Dyes Bearing Fluorenone Acceptor for Dye Sensitized Solar Cells. *J. Mol. Struct.* **2021**, *1226*, 129367. https://doi.org/10.1016/j.molstruc.2020.129367.

[12] Jain, N.; Mary, A.; Dalal, P. M.; Sakla, R.; Jose, D. A.; Jain, M.; Naziruddin, A. R., Ruthenium Complexes Bearing Bis - N -heterocyclic Carbene Donors in TiO_2 Sensitization for Dye-Sensitized Solar Cells. *Eur. J. Inorg. Chem.* **2022**, *2022* (35). https://doi.org/10.1002/ejic.202200502.

[13] Casarin, L.; Swords, W. B.; Caramori, S.; Bignozzi, C. A.; Meyer, G. J., Rapid Static Sensitizer Regeneration Enabled by Ion Pairing. *Inorg. Chem.* **2017**, *56* (13), 7324-7327. https://doi.org/10.1021/acs.inorgchem.7b00819.

[14] Parlane, F. G. L.; Mustoe, C.; Kellett, C. W.; Simon, S. J.; Swords, W. B.; Meyer, G. J.; Kennepohl, P.; Berlinguette, C. P., Spectroscopic Detection of Halogen Bonding Resolves Dye Regeneration in the Dye-Sensitized Solar Cell. *Nat. Commun.* **2017**, *8* (1), 1761. https://doi.org/10.1038/s41467-017-01726-7.

[15] Mathew, S.; Yella, A.; Gao, P.; Humphry-Baker, R.; Curchod, B. F. E.; Ashari-Astani, N.; Tavernelli, I.; Rothlisberger, U.; Nazeeruddin, M. K.; Grätzel, M., Dye-Sensitized Solar Cells with 13% Efficiency Achieved through the Molecular Engineering of Porphyrin Sensitizers. *Nat. Chem.* **2014**, *6* (3), 242–247. https://doi.org/10.1038/nchem.1861.

[16] Muñoz-García, A. B.; Benesperi, I.; Boschloo, G.; Concepcion, J. J.; Delcamp, J. H.; Gibson, E. A.; Meyer, G. J.; Pavone, M.; Pettersson, H.; Hagfeldt, A.; Freitag, M., Dye-Sensitized Solar Cells Strike Back. *Chem. Soc. Rev.* **2021**, *50* (22), 12450-12550. https://doi.org/10.1039/D0CS01336F.

[17] Rui, H.; Shen, J.; Yu, Z.; Li, L.; Han, H.; Sun, L., Stable Dye-Sensitized Solar Cells Based on Copper(II/I) Redox Mediators Bearing a Pentadentate Ligand. *Angew. Chemie Int. Ed.* **2021**, *60* (29), 16156-16163. https://doi.org/10.1002/anie.202104563.

[18] Obiyenwa, G. K.; Semire, B.; Oyebamiji, A. K.; Abdulsalami, I. O.; Latona, D. F.; Adeoye, M. D.; Odunola, O. A., TD-DFT and DFT Investigation on Electrons Transporting Efficiency of 2-Cyano-2-Pyran-4-Ylidene-Acetic Acid and 2-Cyanoprop-2-Enoic Acid as Acceptors for Thiophene-Based π-Linkers Dye-Sensitized Solar Cells. *Eurasian J. Chem.* **2023**, *111* (3), 69-82. https://doi.org/10.31489/2959-0663/3-23-9.

[19] Janjua, M. R. S. A.; Khan, M. U.; Khalid, M.; Ullah, N.; Kalgaonkar, R.; Alnoaimi, K.; Baqader, N.; Jamil, S., Theoretical and Conceptual Framework to Design Efficient Dye-Sensitized Solar Cells (DSSCs): Molecular Engineering by DFT Method. *J. Clust. Sci.* **2021**, *32* (2), 243-253. https://doi.org/10.1007/s10876-020-01783-x.

[20] Sampaio, R. N.; Piechota, E. J.; Troian-Gautier, L.; Maurer, A. B.; Hu, K.; Schauer, P. A.; Blair, A. D.; Berlinguette, C. P.; Meyer, G. J., Kinetics Teach That Electronic Coupling Lowers the Free-Energy Change That Accompanies Electron Transfer. *Proc. Natl. Acad. Sci.* **2018**, *115* (28), 7248-7253. https://doi.org/10.1073/pnas.1722401115.

[21] Piechota, E. J.; Sampaio, R. N.; Troian-Gautier, L.; Maurer, A. B.; Berlinguette, C. P.; Meyer, G. J., Entropic Barriers Determine Adiabatic Electron Transfer Equilibrium. *J. Phys. Chem. C* **2019**, *123* (6), 3416-3425. https://doi.org/10.1021/acs.jpcc.8b11815.

[22] Zhu, W.; Wu, Y.; Wang, S.; Li, W.; Li, X.; Chen, J.; Wang, Z. S.; Tian, H., Organic D-A-π-A Solar Cell Sensitizers with Improved Stability and Spectral Response. *Adv. Funct. Mater.* **2011**, *21* (4), 756-763. https://doi.org/10.1002/adfm.201001801.

[23] Zhang, M. D.; Xie, H. X.; Ju, X. H.; Qin, L.; Yang, Q. X.; Zheng, H. G.; Zhou, X. F., D-D-π-A Organic Dyes Containing 4,4′-Di(2-Thienyl)Triphenylamine Moiety for Efficient Dye-Sensitized Solar Cells. *Phys. Chem. Chem. Phys.* **2013**, *15* (2), 634-641. https://doi.org/10.1039/c2cp42993d.

[24] Lee, M. -W.; Kim, J. -Y.; Son, H. J.; Kim, J. Y.; Kim, B.; Kim, H.; Lee, D. -K.; Kim, K.; Lee, D. -H.; Ko, M. J., Tailoring of Energy Levels in D-π-A Organic Dyes via Fluorination of Acceptor Units for Efficient Dye-Sensitized Solar Cells. *Sci. Rep.* **2015**, *5* (1), 7711. https://doi.org/10.1038/srep07711.

[25] Li, Y.; Sun, C.; Qi, D.; Song, P.; Ma, F., Effects of Different Functional Groups on the Optical and Charge Transport Properties of Copolymers for Polymer Solar Cells. *RSC Adv.* **2016**, *6* (66), 61809-61820. https://doi.org/10.1039/C6RA07647E.

[26] Suresh, T.; Chitumalla, R. K.; Hai, N. T.; Jang, J.; Lee, T. J.; Kim, J. H., Impact of Neutral and Anion Anchoring Groups on the Photovoltaic Performance of Triphenylamine Sensitizers for Dye-Sensitized Solar Cells. *RSC Adv.* **2016**, *6* (32), 26559-26567. https://doi.org/10.1039/C6RA00636A.

[27] Nazeeruddin, M. K.; De Angelis, F.; Fantacci, S.; Selloni, A.; Viscardi, G.; Liska, P.; Ito, S.; Takeru, B.; Grätzel, M., Combined Experimental and DFT-TDDFT Computational Study of Photoelectrochemical Cell Ruthenium Sensitizers. *J. Am. Chem. Soc.* **2005**, *127* (48), 16835-16847. https://doi.org/10.1021/ja052467l.

[28] Kumar, C. V.; Raptis, D.; Koukaras, E. N.; Sygellou, L.; Lianos, P., Study of an Indoline–Phenothiazine Based Organic Dye for Dye-Sensitized Solar Cells. Theoretical Calculations and Experimental Data. *Org. Electron.* **2015**, *25*, 66-73. https://doi.org/10.1016/j.orgel.2015.06.009.

[29] Li, M.; Kou, L.; Diao, L.; Zhang, Q.; Li, Z.; Wu, Q.; Lu, W.; Pan, D., Theoretical Study of Acene-Bridged Dyes for Dye-Sensitized Solar Cells. *J. Phys. Chem. A* **2015**, *119* (13), 3299-3309. https://doi.org/10.1021/acs.jpca.5b00798.

[30] Iqbal, Z.; Wu, W. Q.; Zhang, H.; Han, L.; Fang, X.; Wang, L.; Kuang, D. Bin; Meier, H.; Cao, D., Influence of Spatial Arrangements of π-Spacer and Acceptor of Phenothiazine Based Dyes on the Performance of Dye-Sensitized Solar Cells. *Org. Electron.* **2013**, *14* (10), 2662-2672. https://doi.org/10.1016/j.orgel.2013.07.007.

[31] Munusamy, A. P.; Ammasi, A.; Shajahan, S.; Ahamad, T.; Khan, M. A. M., Quantum Chemical Investigation on D-π-A-Based Phenothiazine Organic Chromophores with Spacer and Electron Acceptor Effects for DSSCs. *Struct. Chem.* **2021**, *32* (6), 2199-2207. https://doi.org/10.1007/s11224-021-01787-x.

[32] Agrawal, S.; Pastore, M.; Marotta, G.; Reddy, M. A.; Chandrasekharam, M.; De Angelis, F., Optical Properties and Aggregation of Phenothiazine-Based Dye-Sensitizers for Solar Cells Applications: A Combined Experimental and Computational Investigation. *The Journal of Physical Chemistry C* **2013**, *117* (19), 9613-9622. https://doi.org/10.1021/jp4026305.

[33] Wan, Z.; Jia, C.; Duan, Y.; Zhou, L.; Lin, Y.; Shi, Y., Phenothiazine–Triphenylamine Based Organic Dyes Containing Various Conjugated Linkers for Efficient Dye-Sensitized Solar Cells. *J. Mater. Chem.* **2012**, *22* (48), 25140. https://doi.org/10.1039/c2jm34682f.

[34] Kim, M. -J.; Yu, Y. -J.; Kim, J. -H.; Jung, Y. -S.; Kay, K. -Y.; Ko, S. -B.; Lee, C. -R.; Jang, I. -H.; Kwon, Y. -U.; Park, N. -G., Tuning of Spacer Groups in Organic Dyes for Efficient Inhibition of Charge Recombination in Dye-Sensitized Solar Cells. *Dye. Pigment.* **2012**, *95* (1), 134-141. https://doi.org/10.1016/j.dyepig.2012.04.002.

[35] Iqbal, Z.; Wu, W. Q.; Kuang, D. Bin; Wang, L.; Meier, H.; Cao, D., Phenothiazine-Based Dyes with Bilateral Extension of π-Conjugation for Efficient Dye-Sensitized Solar Cells. *Dye. Pigment.* **2013**, *96* (3), 722-731. https://doi.org/10.1016/j.dyepig.2012.11.010.

[36] Wu, W.; Yang, J.; Hua, J.; Tang, J.; Zhang, L.; Long, Y.; Tian, H., Efficient and Stable Dye-Sensitized Solar Cells Based on Phenothiazine Sensitizers with Thiophene Units. *J. Mater. Chem.* **2010**, *20* (9), 1772. https://doi.org/10.1039/b918282a.

[37] Tian, Y.; Ying, X.; Zhou, C.; Zhang, S.; Zhao, S.; Li, K.; Xu, M.; Yu, H. J.; Shao, G.; Fang, J. K., Novel Organic Dyes for Dye-Sensitized Solar Cells Based on 1-(2-Ethylhexyl)Pyrrole as a π-Bridge. *Dye. Pigment.* **2020**, *182*. https://doi.org/10.1016/j.dyepig.2020.108655.

[38] Dhar, A.; Kumar, N. S.; Ibrahim, A. A.; Vekariya, R. L., Effective Photo-Harvesting by Dye Sensitized Solar Cell Based on Dihydrothieno [3,4-b][1,4] Dioxine Bridge Based Metal Free Organic Dye. *Org. Electron.* **2018**, *56*, 232-239. https://doi.org/10.1016/j.orgel.2018.02.022.

[39] Wu, Z. -S.; Song, X. -C.; Liu, Y. -D.; Zhang, J.; Wang, H. -S.; Chen, Z. -J.; Liu, S.; Weng, Q.; An, Z. -W.; Guo, W. -J., New Organic Dyes with Varied Arylamine Donors as Effective Co-Sensitizers for Ruthenium Complex N719 in Dye Sensitized Solar Cells. *J. Power Sources* **2020**, *451*, 227776. https://doi.org/10.1016/j.jpowsour.2020.227776.

[40] Tan, H.; Pan, C.; Wang, G.; Wu, Y.; Zhang, Y.; Zou, Y.; Yu, G.; Zhang, M., Phenoxazine-Based Organic Dyes

with Different Chromophores for Dye-Sensitized Solar Cells. *Org. Electron.* **2013**, *14* (11), 2795-2801. https://doi.org/10.1016/j.orgel.2013.07.008.

[41] Roohi, H.; Mohtamadifar, N., The Role of the Donor Group and Electron-Accepting Substitutions Inserted in π-Linkers in Tuning the Optoelectronic Properties of D-π-A Dye-Sensitized Solar Cells: A DFT/TDDFT Study. *RSC Adv.* **2022**, *12* (18), 11557-11573. https://doi.org/10.1039/d2ra00906d.

[42] Semire, B.; Obiyenwa, K. G.; Anthony, W. O.; Abubakar, K.; Godwin, M. A.; Fagbenro, S. O.; Olusegun, S., Manipulation of 2-[2-(10H-phenothiazin-3-yl)thiophen-3-yl]-10 H -Phenothiazine Based D-A-π-A Dyes for Effective Tuning of Optoelectronic Properties and Intramolecular Charge Transfer in Dye Sensitized Solar Cells : A DFT/TD-DFT Approach. *Adv. J. Chem. A* **2024**, *7*, 41-58. https://doi.org/10.48309/ajca.2024.412442.1400.

[43] Ha, N. V.; Dat, D. T.; Nguyet, T. T., Stereoelectronic Properties of 1,2,4-Triazole-Derived N-Heterocyclic Carbenes-A Theoretical Study. *VNU J. Sci. Nat. Sci. Technol.* **2019**, *35* (4). https://doi.org/10.25073/2588-1140/vnunst.4935.

[44] Jacquemin, D.; Brémond, E.; Planchat, A.; Ciofini, I.; Adamo, C., TD-DFT Vibronic Couplings in Anthraquinones: From Basis Set and Functional Benchmarks to Applications for Industrial Dyes. *J. Chem. Theory Comput.* **2011**, *7* (6), 1882-1892. https://doi.org/10.1021/ct200259k.

[45] Tirri, B.; Mazzone, G.; Ottochian, A.; Gomar, J.; Raucci, U.; Adamo, C.; Ciofini, I. A., A combined Monte Carlo/DFT approach to simulate UV-Vis spectra of molecules and aggregates: Merocyanine dyes as a case study. *Journal of Computational Chemistry* **2021**, *42* (15), 1054-1063. https://doi.org/10.1002/jcc.26505.

[46] Delgado-Montiel, T.; Soto-Rojo, R.; Baldenebro-López, J.; Glossman-Mitnik, D., Theoretical Study of the Effect of Different π Bridges Including an Azomethine Group in Triphenylamine-Based Dye for Dye-Sensitized Solar Cells. *Molecules* **2019**, *24* (21), 3897. https://doi.org/10.3390/molecules24213897.

[47] Pearson, R. G., Absolute Electronegativity and Hardness: Application to Inorganic Chemistry. *Inorg. Chem.* **1988**, *27* (4), 734-740. https://doi.org/10.1021/ic00277a030.

[48] Khanmohammadi Chenab, K.; Sohrabi, B.; Zamani Meymian, M. R.; Mousavi, S. V., Naphthoquinone Derivative-Based Dye for Dye-Sensitized Solar Cells: Experimental and Computational Aspects. *Mater. Res. Express* **2019**, *6* (8), 085537. https://doi.org/10.1088/2053-1591/ab2500.

[49] Sun, C.; Li, Y.; Song, P.; Ma, F., An Experimental and Theoretical Investigation of the Electronic Structures and Photoelectrical Properties of Ethyl Red and Carminic Acid for DSSC Application. *Materials (Basel).* **2016**, *9* (10), 1-22. https://doi.org/10.3390/ma9100813.

[50] Amkassou, A.; Zgou, H., New Dyes for DSSC Containing Thienylen-Phenylene: A Theoretical Investigation. *Mater. Today Proc.* **2019**, *13*, 569-578. https://doi.org/10.1016/j.matpr.2019.04.015.

[51] Sharmoukh, W.; Hassan, Z. M.; Ali, B. A.; Elnagar, M. M.; Abdo, R. M.; Allam, N. K., Position of the Anchoring Group Determined the Sensitization Efficiency of Metal-Free D-π-A Dyes: Combined Experimental and TD-DFT Insights. *J. Photochem. Photobiol. A Chem.* **2018**, *367*, 128-136. https://doi.org/10.1016/j.jphotochem.2018.08.034.

[52] Shi, X.; Yang, Y.; Wang, L.; Li, Y., Introducing Asymmetry Induced by Benzene Substitution in a Rigid Fused π Spacer of D-π-A-Type Solar Cells: A Computational Investigation. *J. Phys. Chem. C* **2019**, *123* (7), 4007-4021. https://doi.org/10.1021/acs.jpcc.8b10963.

[53] Kzar Al-Masoodi, K. O.; Rafiq, I.; Assyry, A. El; Derouiche, A., DFT/TD-DFT Study of Donorπ-Acceptor Organic Dye Models Contained Triarylamine for an Efficient Dye-Sensitized Solar Cell. *J. Phys. Conf. Ser.* **2021**, *1963* (1), 012012. https://doi.org/10.1088/1742-6596/1963/1/012012.

[54] Kacimi, R.; Raftani, M.; Abram, T.; Azaid, A.; Ziyat, H.; Bejjit, L.; Bennani, M. N.; Bouachrine, M., Theoretical Design of D-π-A System New Dyes Candidate for DSSC Application. *Heliyon* **2021**, *7* (6), e07171. https://doi.org/10.1016/j.heliyon.2021.e07171.

[55] Zhang, C. -R.; Liu, Z. -J.; Chen, Y. -H.; Chen, H. -S.; Wu, Y. -Z.; Feng, W.; Wang, D. -B., DFT and TD-DFT Study on Structure and Properties of Organic Dye Sensitizer TA-St-CA. *Curr. Appl. Phys.* **2010**, *10* (1), 77-

83. https://doi.org/10.1016/j.cap.2009.04.018.

[56] Hutchison, G. R.; Ratner, M. A.; Marks, T. J., Hopping Transport in Conductive Heterocyclic Oligomers: Reorganization Energies and Substituent Effects. *J. Am. Chem. Soc.* **2005**, *127* (7), 2339-2350. https://doi.org/10.1021/ja0461421.

[57] Bourass, M.; Touimi Benjelloun, A.; Benzakour, M.; Mcharfi, M.; Hamidi, M.; Bouzzine, S. M.; Serein-Spirau, F.; Jarrosson, T.; Sotiropoulos, J. M.; Bouachrine, M., The Optoelectronic Properties of New Dyes Based on Thienopyrazine. *Comptes Rendus Chim.* **2017**, *20* (5), 461-466. https://doi.org/10.1016/j.crci.2016.12.004.

[58] Semire, B.; Afolabi, S. O.; Latona, D. F.; Oyebamiji, A. K.; Adeoye, M. D.; Owonikoko, A. D.; Oyebamiji, O. M.; Abdulsalami, I. O.; Odunola, O. A., Quantum Chemical Elucidation on the Optoelectronic Properties of N2-(4-Aminophenyl)Pyridine-2,5-Diamine Based Dyes for Solar Cells Utilization. *Chem. Africa* **2023**, *6* (5), 2649-2663. https://doi.org/10.1007/s42250-023-00674-8.

[59] Deogratias, G.; Seriani, N.; Pogrebnaya, T.; Pogrebnoi, A., Tuning Optoelectronic Properties of Triphenylamine Based Dyes through Variation of Pi-Conjugated Units and Anchoring Groups: A DFT/TD-DFT Investigation. *J. Mol. Graph. Model.* **2020**, *94*, 107480. https://doi.org/10.1016/j.jmgm.2019.107480.

[60] Bourass, M.; Benjelloun, A. T.; Benzakour, M.; Mcharfi, M.; Hamidi, M.; Bouzzine, S. M.; Bouachrine, M., DFT and TD-DFT Calculation of New Thienopyrazine-Based Small Molecules for Organic Solar Cells. *Chem. Cent. J.* **2016**, *10* (1), 1-11. https://doi.org/10.1186/s13065-016-0216-6.

[61] Javed, M.; Farhat, A.; Jabeen, S.; Khera, R. A.; Khalid, M.; Iqbal, J., Optoelectronic Properties of Naphthalene Bis-Benzimidazole Based Derivatives and Their Photovoltaic Applications. *Comput. Theor. Chem.* **2021**, *1204* (July), 113373. https://doi.org/10.1016/j.comptc.2021.113373.

[62] Vuai, S. A. H.; Khalfan, M. S.; Babu, N. S., DFT and TD-DFT Studies for Optoelectronic Properties of Coumarin Based Donor-π-Acceptor (D-π-A) Dyes: Applications in Dye-Sensitized Solar Cells (DSSCS). *Heliyon* **2021**, *7* (11), e08339. https://doi.org/10.1016/j.heliyon.2021.e08339.

[63] Delgado-Montiel, T.; Baldenebro-López, J.; Soto-Rojo, R.; Glossman-Mitnik, D., Theoretical Study of the Effect of π-Bridge on Optical and Electronic Properties of Carbazole-Based Sensitizers for DSSCs. *Molecules* **2020**, *25* (16). https://doi.org/10.3390/molecules25163670.

[64] Zhang, X.; Gou, F.; Shi, J.; Gao, H.; Xu, C.; Zhu, Z.; Jing, H., Molecular Engineering of New Phenothiazine-Based D-A-π-A Dyes for Dye-Sensitized Solar Cells. *RSC Adv.* **2016**, *6* (108), 106380-106386. https://doi.org/10.1039/C6RA20769C.

[65] Jafari Chermahini, Z.; Najafi Chermahini, A., Theoretical Study on the Bridge Comparison of TiO2 Nanoparticle Sensitizers Based on Phenoxazine in Dye-Sensitized Solar Cells. *Theor. Chem. Acc.* **2017**, *136* (3), 34. https://doi.org/10.1007/s00214-017-2063-5.

[66] Ding, W. -L.; Wang, D. -M.; Geng, Z. -Y.; Zhao, X. -L.; Xu, W. -B., Density Functional Theory Characterization and Verification of High-Performance Indoline Dyes with D-A-π-A Architecture for Dye-Sensitized Solar Cells. *Dye. Pigment.* **2013**, *98* (1), 125-135. https://doi.org/10.1016/j.dyepig.2013.02.008.

[67] Chitpakdee, C.; Namuangruk, S.; Suttisintong, K.; Jungsuttiwong, S.; Keawin, T.; Sudyoadsuk, T.; Sirithip, K.; Promarak, V.; Kungwan, N., Effects of π-Linker, Anchoring Group and Capped Carbazole at Meso-Substituted Zinc-Porphyrins on Conversion Efficiency of DSSCs. *Dye. Pigment.* **2015**, *118*, 64-75. https://doi.org/10.1016/j.dyepig.2015.03.002.

[68] Bouzineb, Y.; Slimi, A.; Raftani, M.; Fitri, A.; Benjelloun, A. T.; Benzakour, M.; Mcharfi, M.; Bouachrine, M., Theoretical Study of Organic Sensitizers Based on 2,6-Diphenyl-4H-Pyranylidene/1,3,4-Oxadiazole for Dye-Sensitized Solar Cells. *J. Mol. Model.* **2020**, *26* (12), 346. https://doi.org/10.1007/s00894-020-04611-1.

[69] Rajan, V. K.; Muraleedharan, K., A Computational Investigation on the Structure, Global Parameters and Antioxidant Capacity of a Polyphenol, Gallic Acid. *Food Chem.* **2017**, *220*, 93-99. https://doi.org/10.1016/j.foodchem.2016.09.178.

[70] Kumar, M. D.; Rajesh, P.; Dharsini, R. P.; Inban, M. E., Molecular Geometry, NLO, MEP, HOMO-LUMO and Mulliken Charges of Substituted Piperidine Phenyl Hydrazines by Using Density Functional Theory. *Asian J. Chem.* **2020**, *32* (2), 401-407.

https://doi.org/10.14233/ajchem.2020.22444.

[71] Raftani, M.; Abram, T.; Bennani, N.; Bouachrine, M., Theoretical Study of New Conjugated Compounds with a Low Bandgap for Bulk Heterojunction Solar Cells: DFT and TD-DFT Study. *Results Chem.* **2020**, *2*, 100040. https://doi.org/10.1016/j.rechem.2020.100040.

[72] Ranjitha, S.; Rajarajan, G.; Gnanendra, T. S.; Anbarasan, P M.; Aroulmoji, V., Structural and Optical Properties of Purpurin for Dye-Sensitized Solar Cells. *Spectrochim. Acta-Part A Mol. Biomol. Spectrosc.* **2015**, *149*, 997-1008. https://doi.org/10.1016/j.saa.2015.04.046.

[73] Islam, A.; Sugihara, H.; Arakawa, H., Molecular Design of Ruthenium(II) Polypyridyl Photosensitizers for Efficient Nanocrystalline TiO_2 Solar Cells. *J. Photochem. Photobiol. A Chem.* **2003**, *158* (2-3), 131-138. https://doi.org/10.1016/S1010-6030(03)00027-3.

[74] Arunkumar, A.; Shanavas, S.; Acevedo, R.; Anbarasan, P. M., Computational Analysis on D-π-A Based Perylene Organic Efficient Sensitizer in Dye-Sensitized Solar Cells. *Opt. Quantum Electron.* **2020**, *52* (3), 164. https://doi.org/10.1007/s11082-020-02273-0.

[75] Soto-Rojo, R.; Baldenebro-López, J.; Glossman-Mitnik, D., Study of Chemical Reactivity in Relation to Experimental Parameters of Efficiency in Coumarin Derivatives for Dye Sensitized Solar Cells Using DFT. *Phys. Chem. Chem. Phys.* **2015**, *17* (21), 14122-14129. https://doi.org/10.1039/C5CP01387A.

[76] Hutchison, G. R.; Ratner, M. A.; Marks, T. J., Hopping Transport in Conductive Heterocyclic Oligomers: Reorganization Energies and Substituent Effects. *J. Am. Chem. Soc.* **2005**, *127* (7), 2339-2350. https://doi.org/10.1021/ja0461421.